HHS Public Access

Author manuscript

Biomaterials. Author manuscript; available in PMC 2017 March 01.

Published in final edited form as:

Biomaterials. 2016 March ; 81: 169–180. doi:10.1016/j.biomaterials.2015.12.009.

Tissue plasminogen activator followed by antioxidant-loaded nanoparticle delivery promotes activation/mobilization of progenitor cells in infarcted rat brain

Marianne Petro, B.S.[*], **Hayder Jaffer, MD**[*], **Jun Yang, MD**[*], **Shushi Kabu, MS**[*], **Viola B. Morris, Ph.D.**, and **Vinod Labhasetwar, PhD**[§]

Department of Biomedical Engineering, Lerner Research Institute, Cleveland Clinic, Cleveland, OH 44195

Abstract

Inherent neuronal and circulating progenitor cells play important roles in facilitating neuronal and functional recovery post stroke. However, this endogenous repair process is rather limited, primarily due to unfavorable conditions in the infarcted brain involving reactive oxygen species (ROS)-mediated oxidative stress and inflammation following ischemia/reperfusion injury. We hypothesized that during reperfusion, effective delivery of antioxidants to ischemic brain would create an environment without such oxidative stress and inflammation, thus promoting activation and mobilization of progenitor cells in the infarcted brain. We administered recombinant human tissue-type plasminogen activator (tPA) via carotid artery at 3 h post stroke in a thromboembolic rat model, followed by sequential administration of the antioxidants catalase (CAT) and superoxide dismutase (SOD), encapsulated in biodegradable nanoparticles (nano-CAT/SOD). Brains were harvested at 48 h post stroke for immunohistochemical analysis. Ipsilateral brain slices from animals that had received tPA + nano-CAT/SOD showed a widespread distribution of glial fibrillary acidic protein-positive cells (with morphology resembling radial glia-like neural precursor cells) and nestin-positive cells (indicating the presence of immature neurons); such cells were considerably fewer in untreated animals or those treated with tPA alone. Brain sections from animals receiving tPA + nano-CAT/SOD also showed much greater numbers of SOX2- and nestin-positive progenitor cells migrating from subventricular zone of the lateral ventricle and entering the rostral migratory stream than in t-PA alone treated group or untreated control. Further, animals treated with tPA + nano-CAT/SOD showed far fewer caspase-positive cells and fewer neutrophils than did other groups, as well as an inhibition of hippocampal swelling. These

[§]Author for correspondence: Vinod Labhasetwar, Ph.D., Department of Biomedical Engineering/ND20, Cleveland Clinic, 9500 Euclid Avenue, Cleveland, OH 44195, Tel: 216/445-9364; Fax: 216/444-9198; labhasv@ccf.org.

[*]These authors contributed equally to this work.

Conflict of interest

Dr. Vinod Labhasetwar is Co-Founder and Chief Scientific Officer of ProTransit Nanotherapy (http://www.protransitnanotherapy.com/), a start-up company established based on technology created at the University of Nebraska Medical Center (Omaha, NE), his former institution. If this technology is successful, the author and the University may benefit. The terms of this arrangement are being managed by the Conflict of Interest Committee of Cleveland Clinic in accordance with its conflict of interest policies.

results suggest that the antioxidants mitigated the inflammatory response, protected neuronal cells from undergoing apoptosis, and inhibited edema formation by protecting the blood-brain barrier from ROS-mediated reperfusion injury. A longer-term study would enable us to determine if our approach would assist progenitor cells to undergo neurogenesis and to facilitate neurological and functional recovery following stroke and reperfusion injury.

Keywords

Brain ischemia; Fibrinolytic agents; Intracranial hemorrhages; Nanoparticles; Neurogenesis; Reperfusion injury; Neuronal stem cells; Thrombolytic therapy

1. Introduction

Stroke is the number one cause of long-term disability and the third leading cause of death in the US. Of the two major types of stroke, ischemic and hemorrhagic, ischemic stroke is the more common [1]. It is caused by thrombotic occlusion in a cerebral or carotid artery, resulting in hypoxia that leads to rapid neuronal cell death of parenchyma, creating a stroke epicenter composed of dead tissue (infarct). The poorly perfused tissue surrounding the infarct, the so-called penumbra, is affected by ischemia in a time- and blood flow-dependent manner, thus eventually becoming part of an expanding infarct [2].

Timely intervention is critical to saving the penumbra and minimizing the progression of the infarct [3]; penumbral injury is reversible during the first few hours of ischemia, but only if blood flow is promptly restored [2]. Clinically, reperfusion is achieved by administering the only US FDA-approved treatment for ischemic stroke, recombinant human tissue-type plasminogen activator (the fibrinolytic agent commonly termed tPA). However, treatment with tPA is not safe beyond ~4.5 h post stroke, due to increased risk of hemorrhagic complications, breakdown of the blood-brain barrier (BBB) [4], and neurotoxic effects of tPA [5]; thus only about 5% of patients with ischemic stroke can be treated with this agent today [6]. Although reperfusion after tPA treatment brings oxygen and nutrients to the ischemic tissue, it simultaneously causes increased production of reactive oxygen species (ROS) by ischemic neural and glial cells, infiltrating neutrophils, and vascular cells constituting the BBB [2]. Under normal circumstances, neuronal cells contain high levels of endogenous antioxidants to counteract ROS [7]; these antioxidants are continuously produced during metabolism of excitatory amino acids and neurotransmitters [8]. However, endogenous antioxidants in the ischemic brain cannot attain high enough levels to neutralize the excessive levels of ROS formed during ischemia/reperfusion, resulting in loss of the redox balance and causing oxidative stress [9], which then initiates a cascade of degenerative events such as inflammation, excitotoxicity, hyperglycemia, and apoptosis. This stress condition in turn expands the injury response and infarct volume over time, causing irreversible damage to the brain, especially in the penumbral areas [10].

It was long thought that neurogenesis occurs only in the developing brain; however, some decades ago, *in vitro* studies of brain cells from the subventricular zone (SVZ) showed that these cells have stem-cell properties [11], and more recent studies have given *in vivo* evidence of neurogenesis in adult mammalian brain [12]. It has been shown that endogenous

neural precursor cells (NPCs; i.e., stem cells and progenitor cells) become activated after stroke, then maturate and migrate to the site of injury, where they differentiate into neuronal cells (Fig. 1) [13]. However, this process of neurogenesis is limited, some postulate, because of excessive production of ROS following stroke and reperfusion [14], creating unfavorable conditions for progenitor cells to activate, mobilize, survive, and eventually differentiate into functional neuronal tissue [15]. In fact, Huang *et al*. [16] have shown a marked reduction in neurogenesis in superoxide dismutase (SOD)-deficient mice with radiation-induced brain damage, which also caused a large increase in ROS levels in the injured brain for a sustained period of time.

In this study, we hypothesized that targeting the initial excess of ROS formation with the antioxidant enzymes catalase (CAT) and SOD loaded into nanoparticles (NPs; termed nano-CAT/SOD) at the time of reperfusion (i.e., immediately after tPA delivery) would prevent the ROS-mediated cascade of inflammatory and degenerative events, creating conditions favorable for the activation and mobilization of progenitor cells that could eventually promote the endogenous mechanisms of neurogenesis in the infarcted area.

2. Materials and methods

2.1. Materials

Superoxide dismutase (SOD), catalase (CAT), L-tartaric acid dimethyl ester (dimethyl tartaric acid), rat serum albumin (RSA), thrombin, and polyvinyl alcohol (PVA; average MW, 30 000–70 000) were purchased from Sigma-Aldrich Corp. (St. Louis, MO). The polymer poly (D,L-lactide *co*-glycolide) (PLGA; inherent viscosity, 0.76–0.94 dL/g; copolymer ratio, 50:50) was purchased from LACTEL Absorbable Polymers (DURECT Corp., Cupertino, CA). Dichloromethane was purchased from Thermo Fisher Scientific, Inc. (Pittsburgh, PA).

2.2. Methods

2.2.1. Nanoparticle formulation and characterization—NPs were formulated and characterized as previously described [17, 18]. In brief, we used a double-emulsion solvent-evaporation method in which antioxidant enzymes are encapsulated in the biodegradable polymer PLGA. To formulate CAT-loaded NPs, an aqueous phase containing 8 mg CAT (2,000–5,000 U/mg) and 22 mg RSA in 300 μl of double-distilled water was used. For SOD-loaded NPs, an aqueous phase containing 12 mg SOD (activity >3 000 U/mg, from bovine erythrocytes) and 18 mg RSA in 300 μl of double-distilled water was used. The aqueous phase was emulsified into a polymer phase containing PLGA (81 mg) and dimethyl tartaric acid (9 mg) dissolved in 3 ml dichloromethane to form a water-in-oil (w/o) emulsion. The emulsification was achieved first by vortexing, followed by sonication for 2 min on an ice bath using a microtip probe sonicator set at 55 W of energy output (XL 2015 Sonicator® Ultrasonic Processor, Misonix, Inc., Farmingdale, NY). The primary emulsion was further emulsified into an aqueous phase containing 18 ml of 3% w/v PVA solution in water to form a water-in-oil-in-water (w/o/w) emulsion using the above procedure of vortexing followed by sonication. The PVA solution was filtered through a 0.22-μm syringe filter (MILLEX® GP Syringe Filter unit, Millipore Ireland Ltd., Carrigtwohill, Ireland) prior to use. The

emulsion was stirred on a magnetic stir plate overnight to evaporate any organic solvent. The formed NPs were recovered by ultracentrifugation, washed to remove unencapsulated enzymes and PVA, and lyophilized for 48 h. SOD- and CAT-loaded NPs were formulated separately using an identical protocol. The size and charge of NPs were measured with a NICOMP™ 380 ZLS Zeta Potential/Particle Sizer (Particle Sizing Systems, Port Richey, FL). The loading efficiency of each enzyme was determined by subtracting the nonencapsulated enzyme activity (found in supernatants from washing steps during preparation) from total enzyme activity added to the formulation.

2.2.2. Animal studies—Male Sprague-Dawley rats (400–425 g) were purchased from Harlan Laboratories, Inc. (Indianapolis, IN). All animal procedures were approved by Cleveland Clinic's Institutional Animal Care and Use Committee, and animals received humane care and treatment according to federal and institutional guidelines.

2.2.3. Thromboembolic stroke induction—Stroke was induced as per our previously described procedure [19]. In brief, the right common carotid artery, external carotid artery (ECA), and internal carotid artery (ICA) were exposed. The ECA was ligated with a suture at the distal end and temporarily occluded with a clip at the proximal end. A small incision, very close to the distal end, was made in the ECA wall. A catheter was loaded with thrombin (25 μl), inserted through the ECA and slowly advanced into the ICA, and then secured with a suture. Arterial blood was allowed to interact with thrombin within the catheter for 20 min to form a clot. The right and left carotid arteries were temporarily occluded with clips, and the clot was injected slowly over 1 min. The left carotid artery was released after 10 min of clot injection and the right after 15 min. The catheter was left in place to be used for future delivery of treatment, as described below. The wound was sutured, and the animals were allowed to recover. Control animals without induced stroke underwent surgery for right ICA catheterization as described above but were injected with 20 μl normal saline. Using the above method, the average infarct volume as determined previously was 23 ± 2% (mean ± s.e.m., n = 10) [19].

2.2.4. Treatments—There were four experimental groups in this study: untreated animals with stroke; animals receiving tPA only at 3 h post stroke; animals receiving tPA + nano-CAT/SOD at 3 h post stroke; and naïve animals (no stroke). Applicable treatments were given separately 3 h post stroke induction via the ICA catheter. The tPA (Activase® [alteplase], Genentech, San Francisco, CA) was delivered first (2 mg/kg), followed by NPs loaded with CAT, and lastly NPs loaded with SOD. The catheter was rinsed with 20 μl normal saline for over 1 min after each treatment injection. First, a bolus of 10% of the total tPA dose was administered; the remaining tPA was then delivered slowly over 40 min using an infusion pump (Harvard Apparatus, Holliston, MA). The concentration of NPs loaded with CAT was 10 mg/ml, and a total dose of 8 mg/kg per rat was given over 1 min. The concentration of NPs loaded with SOD was 10 mg/ml, and a total dose of 4 mg/kg per rat was given over 1 min. The ratio 1:2 w/w for SOD- and CAT-loaded NPs was selected based on the optimal protective effect of the combination in this ratio in hydrogen-peroxide-induced oxidative stress in rat neurons (unpublished data).

2.2.5. Immunohistochemistry—At 48 h post stroke induction, the animals were sedated in an induction chamber with 5% isoflurane and then kept under 2.5% isoflurane with a mask while 20 ml phosphate-buffered saline (PBS) was rinsed through each carotid artery, followed by 10 ml of 10% normal buffered formalin. After harvest, the brains were kept in 10% normal buffered formalin at room temperature for 24 h; they were then placed into PBS and kept at 4 °C until standard processing and embedding in paraffin. Five coronal sections (5 μm) were cut at bregma 1.0 mm to obtain the SVZ and at bregma 4.0 mm to obtain the hippocampus. Sections were deparaffinized and hydrated, and antigen retrieval was done with two repetitions of Trilogy™ pretreatment solution (Cat. No. CMX 833 1CS; Cell Marque, Rocklin, CA) for 30 min each in a conventional food steamer. Slides were then cooled down to room temperature, rinsed in tap water, and put in 0.3% H_2O_2 in 80% methanol for 20 min to block activity of endogenous horseradish peroxidase (HRP). After rinsing with water, slides were then incubated with primary antibody (diluted in Antibody Diluent with Background Reducing Components (S3022; Dako North America, Inc., Carpinteria, CA) for 60 min (anti-Iba1 antibody was incubated for 2.5 h) at RT in a humid chamber and then rinsed three times for 5 min each time in PBS. If mouse monoclonal antibodies were used, slides were incubated with Protein Block Serum-Free (X0909; Dako) for 10 min first. Then either a10-min incubation with HRP-labeled Rb SuperPicTure polymer (SuperPicTure™ Polymer Detection Kit, Cat. No. 87–9263; Invitrogen, Life Technologies, Grand Island, NY) was used for rabbit primary antibodies or a 30-min incubation with HRP-labeled goat anti-mouse IgG polymer (Cat. No. 87-9999; Invitrogen) was used for mouse primary antibodies. Slides were rinsed twice for 5 min each time in PBS and the targeted markers were then visualized with the HRP substrate 3,3′-diaminobenzidine (DAB) prepared as instructed in Invitrogen's kit (Cat. No. 87-9999). For Rb anti-myeloperoxidase (MPO) antibody, we used DAB from a DAB Peroxidase (HRP) Substrate Kit SK-4100 with nickel (Vector Laboratories, Burlingame, CA). Slides were counterstained with either hematoxylin or eosin (H&E) to visualize nontargeted cell structures. The presence of stroke-injured cortex on the ipsilateral side of representative sections was confirmed with conventional H&E stain. Markers investigated were nestin for NPCs and immature neurons, GFAP for astrocytes and NPCs, caspase-3 for apoptosis, and MPO for neutrophils. Primary antibodies used to target these markers were mouse monoclonal anti-nestin antibody (2Q178) (Abcam, Cambridge, MA; Cat. No. ab6142, dil. 1:500); Rb polyclonal anti-GFAP (Dako Code No Z 0334, dil. 1:500); Rb polyclonal anti-active caspase-3 (R&D Systems, Minneapolis, MN; Cat. No. AF835, dil. 1:200); Rb polyclonal anti-MPO (Abcam Cat.No. ab65871, dil. 1:50).

For the double immunofluorescence staining, the brain sections were deparaffinized in xylene and rehydrated in steps with decreasing percent ethanol. The sections were then boiled in 10 mM sodium citrate buffer with 0.05% Tween-20 for 30 min to retrieve antigens. After cooling down to room temperature and washing, non-specific binding of antibodies was blocked by incubating sections in 5% serum derived from the same species in which the secondary antibody was produced. The blocked sections were then incubated with primary antibodies in blocking solution overnight at 4 °C. The primary antibodies used were mouse GFAP (1:200, Cat# 3670, Cell Signaling Technology, Inc., Danvers, MA) combined with rabbit NeuN (1:200, Cat# ab177487, Abcam, Cambridge, MA) or rabbit SOX2 (1:100, Cat#

ab92494, Abcam, Cambridge, MA). After washing, slides were incubated with secondary antibody at room temperature for 1 hr. The secondary antibodies used were goat anti-mouse (1:500, Fluro-488, Cat# ab150117, Abcam, Cambridge, MA) and goat anti-rabbit (1:500, Fluro-568, Cat# ab175471, Abcam, Cambridge, MA). After mounting and counterstaining with VECTASHIELD mounting media with DAPI (Cat# H1200, Vector Laboratories, Burlingame, CA), the sections were observed under fluorescence microscope (Leica, MM RXA2, Buffalo Grove, IL).

2.2.6. Quantification of cells and hippocampal swelling—Slides were scanned in a Leica SCN400 scanner (Leica Biosystems, Buffalo Grove, IL) at 20x magnification for quantification of neutrophils and positive stained cells, Two types of brain sections were used, one cut at the hippocampal level and another to visualize the SVZ. Four regions from the brain were chosen, namely, hippocampus, thalamus, cortex and striatum, which primarily encompassed the ischemic core and penumbra. Four adjacent and equally sized areas (1 mm^2) were taken from each brain region being evaluated, and positive cells were manually counted. Counting was performed for all groups, i.e., naïve, untreated, tPA alone and nano-CAT/SOD. For quantification of hippocampal swelling, scanned images comprising the overview of the entire brain section were chosen. The total area of the hippocampus on the contralateral and ipsilateral sides was measured using Image J (National Institutes of Health, Bethesda, MD), and the ratio was compared between all treated and untreated groups.

2.2.7. Statistical analysis—Statistical significance was calculated using a one-way analysis of variance with the Newman-Keuls post test for the quantification study on neutrophil and positive stained cell counts. Statistical significance for the cell counting and hippocampal swelling study was calculated using *t*-test, and a p value of ≤ 0.05 was considered significant.

3. Results

Enzyme-loaded NPs were designed in the size range of 250–270 nm in hydrodynamic diameter with a polydispersity index of ~0.1 and surface charge (zeta potential) of approximately −17 mV. Previous studies have shown a sustained-release profile of the encapsulated enzymes in active form under *in vitro* simulated physiological conditions, biocompatibility with neutron cells and protection from hydrogen peroxide-induced oxidative stress *in vitro* [17, 18]. Immunohistochemical studies were performed on 5-μm-thick coronal sections from paraffin-embedded rat brains harvested 48 h post induction of thromboembolic stroke.

3.1. GFAP expression in astrocytes, neural progenitor cells (NPCs) and radial glia-like (RGL) cells after stroke

Glial fibrillary acidic protein (GFAP) is the most commonly used marker for astrocytes, but it is also expressed by NPCs and redial glia-like (RGL) cells [20]. After stroke, the ipsilateral side of the cortex (Fig. 2B–c) showed astrocytosis, as evidenced by the short, thickened processes and by increased GFAP expression; the contralateral side (Fig. 2B–a) showed normal star-shaped astrocyte morphology. In addition to astrocytosis on the

ipsilateral side, brains of the rats treated with tPA alone or with tPA + nano-CAT/SOD showed high numbers of strongly stained GFAP-positive cells lacking astrocytic morphology: one group comprised small, round cells with no protrusions, that is progenitor cells (blue arrows) (Fig. 2A–c and d); the other group comprised long, stretched cells with irregular (often triangle-shaped) cell bodies and long protrusions with morphology of RGL cells (red arrows) (Fig. 2A–d). Progenitor cells are more prominent and widespread in the brain sections of animals treated with tPA + nano-CAT/SOD or tPA alone than in the untreated group (Fig. 2A–b vs. c, d). RGL cells, however, were seen only in brains of rats treated with tPA + nano-CAT/SOD, not in the group treated with tPA alone (Fig. 2A–c vs. d).

In addition to observing the cellular morphology, we further elucidated the GFAP positive cells by detecting markers for mature neurons (NeuN) and neural progenitors (SOX2) in the tissues from tPA + nano-CAT/SOD treated animals. GFAP positive cells from the contralateral side showed typical astrocytic morphology as mentioned above, and immunofluorescence double-staining with GFAP and NeuN did not show any double positive cells, suggesting that the GFAP positive cells we see on the contralateral side are astrocytes (Fig. 3A). However, GFAP positive cells on the ipsilateral side of the tPA + nano-CAT/SOD treated animals co-stained for SOX2, suggesting the presence of progenitor cells, for e.g., RGL cells (based on the RGL like morphology of some of the GFAP positive cells) (Fig. 3B).

3.2 Activation and migration of NPCs in the subventricular zone and rostral migratory stream after stroke

In the adult rodent brain, NPCs migrate from the subventricular zone (SVZ) of the lateral ventricle toward the olfactory bulb in a track known as the rostral migratory stream (RMS). These neural precursor cells express Nestin, GFAP, and SOX2, and can be detected using IHC and IF staining methods (Fig. 4). The brain sections of untreated showed increased staining with GFAP, Nestin, and SOX2 in both SVZ and RMS compared with naïve sections, suggesting stroke-induced neurogenesis. However, after treatment with tPA only, the NPCs related staining of SOX2, nestin, and GFAP reduced in RMS, which suggests that tPA alone treatment may result in an unfavorable condition for NPCs migration. Notably, the reduced staining following tPA alone treatment is restored or increased after the treatment with tPA + nano-CAT/SOD. The results suggest that in addition to ROS, tPA hinders in the regeneration progress of the infarcted brain.

3.3. Signs of increased neurogenesis in ipsilateral hemisphere

Nestin, an early marker indicating a progenitor cell's commitment to the neural lineage, was used to stain the brain sections. Brain sections of the ipsilateral hemispheres from naïve, untreated, and tPA alone-treated animals showed little expression of nestin, but sections from animals treated with tPA + nano-CAT/SOD showed a high number of nestin-expressing cells (Fig. 5). Such nestin-positive cells can originate from either inherent residents from SVZ (Fig. 4E) and hippocampus (Fig. 5A) or infiltrating progenitors (Fig. 5B and C). Interestingly, in the animals treated with tPA + nano-CAT/SOD, we noticed that these nestin-positive cells were concentrated around blood vessels (Fig. 5B) and along the

pia mater (Fig. 5C). These nestin-positive cells could either be inherent progenitor cells, or bone marrow derived progenitor cells entering the brain parenchyma from the blood stream. These progenitor cells can be NPCs which has been shown to become activated after stroke and then proliferate and migrate to the site of injury where they differentiate into neuronal cells and/or endothelial progenitor cells. To investigate whether the nestin positive cells are of a neuronal lineage or an endothelial lineage we stained the tissues for the neural progenitor cell marker, SOX2. The result showed not only increase of Nestin positive cells, but also Nestin-SOX2 double positive cells in the group treated with tPA + nano-CAT/SOD, which suggests the possible neurogenesis contributed by NPCs (Fig. 4 and 5).

3.4. Analysis for caspase-3-positive cells and infiltration of neutrophils

The data show decidedly fewer caspase-3-positive cells in the infarcted brains of animals treated with tPA + nano-CAT/SOD than in other groups (Fig. 6A). Similarly, neutrophil infiltration was reduced in certain areas of the brain in the group treated with tPA+ nano-CAT/SOD (Fig. 6B). For example, animals receiving tPA alone or tPA + nano-CAT/SOD showed increased infiltration of neutrophils in the thalamus. It has been known that certain areas of the brain overexpress leukotriene B4 receptors following reperfusion injury, which could result in greater infiltration of neutrophils [21].

3.5. Hippocampal swelling

The ratio of hippocampal area of the ipsilateral vs. contralateral side was used to calculate the relative swelling of the hippocampus on the stroke side. Ipsilateral hippocampal swelling was larger in the untreated animals and in those receiving tPA alone than in those treated with tPA+ nano-CAT/SOD (Fig. 7A). In fact, there was no significant difference in the ratio of hippocampal area between the ipsilateral and contralateral side in animals treated with tPA+ nano-CAT/SOD (Fig. 7B).

4. Discussion

Limiting the size of the infarcted area after ischemic stroke by promoting reperfusion is the first step in counteracting the detrimental effects of a stroke; however, the timing of reperfusion after stroke is critical, since early reperfusion results in better recovery [22]. The next step in recovery is to protect the brain from reperfusion injury to prevent further loss of neurons and glia [23]. Methods to protect the ischemic stroke brain after reperfusion have been investigated in numerous preclinical and clinical studies [24]. Results from clinical trials have not led to any new treatments so far [25], but a growing amount of convincing preclinical data shows that it is possible to protect the brain from reperfusion injury and limit the size of the infarct [26]. Ultimately, the desired outcome in stroke therapy is regeneration of lost brain tissue and reestablishment of neural connectivity.

Working toward the objective of minimizing damage from reperfusion injury and of facilitating recovery, we have been investigating antioxidant-loaded biodegradable NPs [17, 18, 27]. Although the mechanisms leading to neuronal cell death after cerebral ischemia and reperfusion are complex, it is very well known that ROS formation is more pronounced during reperfusion [28] and is considered central to the reperfusion-induced injury leading to

the pathology of stroke [29]. Earlier studies in a rat model of middle cerebral artery occlusion (MCAO) have shown that the infarct volume due to reperfusion injury, depending on the duration of ischemia (120–300 min), could be as high as 72% of the total infarct volume [30]. Mitochondrial dysfunction during ischemia/reperfusion leads to excessive production of ROS, particularly superoxide anions and hydrogen peroxide [31]. SOD can neutralize superoxide, and catalase can neutralize hydrogen peroxide, which is formed due to the dismutation of superoxide anions with SOD [32]; therefore, efficient delivery of the combination of these two enzymes to the brain during reperfusion could minimize damage caused by excessive ROS and also could create conditions conducive to promoting endogenous mechanisms of neurogenesis (Fig. 1).

Various pharmacodynamic factors impede the straightforward use of native forms of antioxidant enzymes because (a) they are rapidly cleared from the systemic circulation ($t_{1/2}$ of SOD in rats = 4–8 min, CAT = 8–10 min); (b) they are negatively charged and therefore do not readily cross the cell membrane [33]; and (c) neuronal cells do not appear to take up the native enzyme and hence cannot neutralize the ROS formed intracellularly. PEGylation and lecithinization improve the circulation half-life [34] of these enzymes, but these modifications also limit their permeability across BBB and uptake by neuronal cells [35].

In our previous study, we demonstrated complete neuroprotection with SOD- and CAT-loaded NPs in an H_2O_2-induced oxidative stress model in human neurons *in vitro*, whereas naïve SOD or CAT and PEGylated SOD in solution were ineffective [18, 27]. The efficacy mentioned above was attributed to the efficient cellular uptake of enzymes encapsulated in NPs that could have also neutralized the ROS formed intracellularly [36]. Further, the encapsulated enzymes are protected from degradation and rapid clearance and show sustained release, which is important since ROS continue to form over several weeks following ischemia/reperfusion [37]. We have previously shown that delivery of SOD-loaded NPs via carotid artery at the time of reperfusion in an MCAO model in rats was significantly more effective in preventing reperfusion injury than SOD in solution or untreated control; treatment with antioxidant NPs mitigated the ROS levels, reduced BBB leakage, and protected neuronal cells from apoptosis, leading to steady neurological recovery with concomitant reduction in infarct volume over 4 weeks [17]. Others have also demonstrated similar efficacy in the MCAO model with antioxidant-loaded NPs [38] and other formulations of NPs that mitigated the ROS levels in the ischemic brain [39].

For the present study, we used a thromboembolic stroke model, and tPA was administered at the time of reperfusion to mimic the clinical scenario, but the results of this study potentially also explain the neuronal recovery seen in our previous study in the MCAO model [17]. The decreased distribution of nestin-positive cells after treatment with tPA alone suggests its inhibitory role in promoting neurogenesis. However, this unfavorable effect of tPA and the excess ROS formed due to ischemia/reperfusion is counteracted following treatment with tPA + nano-CAT/SOD as evidenced from increased distribution of nestin- and SOX2-positive cells. The results of these studies thus indicate that the delivery of tPA + nano-CAT/SOD not only mitigates the inhibitory effect of tPA on neurogenesis but that of ROS formed as a results of ischemia/reperfusion (Fig 4 and 5). Neurogenesis in the post-stroke condition is proposed to occur in various stages [40], with stages 1, 2, and 3 representing

progenitor cell activation, their differentiation, and mobilization, respectively. As discussed below, we detected cells in these three stages of neuronal development in the group treated with tPA + nano-CAT/SOD (Fig 2B–b). Stage 4 is axonal and dendritic targeting, in which immature neurons become post mitotic, and in stage 5, the newly formed neurons establish their synaptic contacts. These last two stages may take several weeks to months to occur and are critical for neuronal and functional recovery. Therefore, a chronic study extending over several weeks would be necessary to determine whether these NPCs actually progress through early stages of neuronal development as seen in our study, whether they continue toward complete neurogenesis, and what impact they have on neuronal and functional recovery.

Neurogenesis after trauma such as ischemic stroke is not limited to the two major neurogenic zones of the normal adult brain, i.e., the dentate gyrus of the hippocampus and the SVZ, but as recent *in vitro* and *in vivo* studies have determined, the neocortical ventricular zone (VZ) contains multiple types of precursors, including several types of RGL cells and short neural precursors [41]. It has been established that VZ precursors can either directly or indirectly give rise to neurons as well as to astrocytes and oligodendrocytes [42]. The maintenance of RGL morphology is critical for proper development; however, because neurons generated from the VZ migrate radially to the cortical plate using these processes as a guide. After the onset of neurogenesis, RGLs generate another specialized cell type, intermediate progenitor cells. These intermediate cells lack both apical endfeet and ascending processes and also differ from RGLs in their gene expression [43]. Thus there are several mechanisms via which neurogenesis could occur following brain trauma [41].

The two major neurogenic zones of the brain, the SVZ and hippocampus, share many similarities; one is the expression of GFAP in RGLs as they transform into progenitor cells. What we noted in the ischemic brains of animals given tPA + nano-CAT/SOD could indicate that cortical pyramidal cells behave in a similar way as RGL cells of the SVZ and the hippocampus (Fig. 2). It is unlikely that the small group of round, strongly GFAP-stained cells we occasionally noted in the cortex of the stroke brain of animals untreated and treated with tPA alone migrated from the SVZ, since we saw no increase, even decrease in migrating nestin- and SOX2-positive cells in the RMS or from the pia mater (Fig. 4, 5), as oxidative stress would not favor that [44]. It is more likely that the nestin-stained cells are blood-/bone-marrow-derived progenitors, entering the parenchyma through the damaged BBB, but unable to proliferate to any great extent or to differentiate and migrate any further, leading to their limited number and sparse focal appearance (around some blood vessels) (Fig. 5B). It is suggested that circulating progenitor cells play a role in the repair mechanism post stroke since their levels in the circulation increase following neuronal injury [45].

Increased numbers of GFAP- (Fig. 2) and SOX2- and nestin-positive (Fig. 4 and 5) cells in the cortex and lateral ventricles suggest that there are increased proliferation of progenitor cells in these areas of brains in both the tPA-only and the tPA + nano-CAT/SOD groups. Yet in brains treated with tPA + nano-CAT/SOD, a greater number of SOX2- and nestin-positive cells were able to migrate into the RMS (Fig. 4). In contrast, in brains of the group receiving tPA alone, these cells remain in the lining of the lateral ventricles and decreased SOX2- and nestin positive cells in RMS [46, 47]. This observation thus suggests that tPA only treatment

could result in environment unfavorable for NPCs migration to RMS, whereas the oxidative-stress-free environment in animals treated with tPA + nano-CAT/SOD might have favored proliferation and migration of progenitor cells from the SVZ to the RMS. Achuta et al. have also shown altered migration and differentiation of NPCs following increased expression of t-PA in glial cells; however, the effect of t-PA was reversed following treatment of cells with antibody against t-PA [48]. Our observation of reduced migration of NPCs in t-PA alone treated animals thus supports the above effect of t-PA (Figure 5). Since our data also show that delivery of tPA along with antioxidant loaded NPs promotes NPCs migration, suggesting that oxidative-stress also contributes to their altered migration of NPCs and also seems to negate the effect of tPA. NPCs in adult rodent brain migrate from the SVZ to the olfactory bulb through the RMS, which has been shown to contain proliferating cells and immature neurons but not mature neurons.

We used the carotid artery for injecting tPA and the nano-CAT/SOD. Some studies have suggested that carotid injection of tPA provides more effective thrombolysis than intravenous injection [49]; others have found no difference but noted an increased risk of hemorrhagic complications [50]. We also found increased vascular leakage, particularly under stroke conditions, when the same dose of tPA was given via carotid artery rather than intravenously in a thromboembolic stroke model in rat [19]. Injecting tPA followed by nano-CAT/SOD via carotid artery, rather than via intravenous injection, could maximize the delivery of antioxidants to the target brain area through the disrupted BBB.

Neuronal cell death after global cerebral ischemia can be attributed to either apoptosis, necrosis, or a combination of both processes [51]. Although the ischemic core is mostly necrotic in nature, various neurons in the ischemic penumbra undergo apoptosis within the first few hours or even up to days after a stroke. Our results from the current study showed a significant decrease in the apoptotic cell numbers in the group treated with tPA + nano-CAT/SOD vs. the group receiving tPA only (Fig. 6A), demonstrating the neuroprotective effect of nano-CAT/SOD.

Following BBB breakdown, immune cells from damaged and disrupted blood vessels infiltrate into the ischemic core, producing inflammatory mediators that further exacerbate edema in the brain, resulting in progression of the infarct lesion [52, 53]. Neutrophils permeate into the ischemic brain within a few hours after the occlusion, reach peak levels within 1–3 days, then continue to decline over time [54, 55]. The exact role of neutrophils in stroke remains debatable, as they are functionally plastic cells known to change their phenotypes *in vivo*, but have conventionally been regarded as instrumental to proliferation of the ischemic injury [55–57]. We noticed relatively lower numbers of neutrophils infiltrating certain areas of the infarcted brain in animals receiving tPA + CAT/SOD than in other groups, suggesting reduced inflammation (Fig. 6B).

Although not determined in this study, it is quite possible that the nano-CAT/SOD protected the BBB from further ROS-mediated damage during reperfusion [58]. This possibility is supported by evidence that showed significantly reduced hippocampal swelling in rats given tPA + nano-CAT/SOD than those given tPA alone (Fig. 7); it is well known that ROS can trigger edema formation following stroke due to BBB breakdown [59, 60]. In our previous

study in the MCAO model, following reperfusion, we showed reduced brain extravasation of Evans Blue dye in post-stroke animals treated with SOD-NPs than in untreated animals. It is known that tPA administration in stroke conditions can further aggravates disruption of the BBB, as shown in our previous study [19] and by others [61]. This disruption causes edema, an urgent and serious issue in stroke, as edema exerts mechanical pressure on the brain. Further, the breakdown of the BBB is also responsible for neuroinflammation and neurodegeneration; thus, protecting its integrity or facilitating its repair is a critical target for therapeutic intervention in stroke [62].

It has been suggested that the process of neurogenesis is regulated by various physiological, pathological and pharmacological stimuli [63]. In this regard, several attempts have been made to induce neurogenesis, such as by exogenous delivery of stem cells or by stimulating proliferation and differentiation of endogenous neuronal progenitor cells with different growth factors [64]. However, the neuronal regeneration process is quite complex, and administration of one or a combination of a few growth factors may not be able to create conditions similar to those required to promote natural mechanisms of regeneration [65]. Our final approach is to provide an option to achieve neuroregeneration through the brain's endogenous repair mechanisms to heal the stroke lesion [26].

In our study, treatment with nano-CAT/SOD could have been effective via multiple mechanisms: by protecting neuronal cells from reperfusion injury, thereby mitigating the inflammatory response; by protecting the BBB, thus preventing edema and infiltration of inflammatory cells; and finally, by creating an environment favorable for the activation and mobilization of progenitor cells that could eventually promote the endogenous mechanisms of neurogenesis in the infarcted area (Fig. 8). Another body of literature suggests that ROS control redox-sensitive signaling pathways and play a role in neuronal differentiation [37]. However, such signaling pathways may be involved as a protective mechanism when the brain suffers from short ischemic episodes that are below the threshold of detectable injury [51, 66].

It is also possible that the activated progenitor cells could promote vascular repair and induce angiogenesis in the infarcted brain, which is also a critical step in brain repair [67]. Further, the protective effect of nano-CAT/SOD may overcome the negative effects of tPA, including its neurotoxic effects, increased vascular leakage, and reperfusion injury, while maintaining its thrombolytic effect. Thus, the sequential administration of tPA followed by nano-CAT/SOD could still be effective even if delayed, because of the neuronal and vascular protective effects of these antioxidants.

5. Conclusion

Our data demonstrate that delivery of nano-CAT/SOD at the time of reperfusion effectively protects neuronal cells, mitigating the inflammatory response and edema formation and promoting activation and mobilization of neuronal and circulating progenitor cells to the infarcted brain. Our overall results suggest that combined treatment with tPA followed by nano-CAT/SOD could facilitate the endogenous process of neurogenesis, potentially resulting in faster neuronal and function recovery post stroke.

Acknowledgments

The study was funded by grant 1R01NS070896 (to VL) from the National Institute of Neurological Disorders and Stroke of the National Institutes of Health.

LIST OF ABBREVIATIONS

BBB	Blood-brain barrier
CAT	Catalase
ECA	External carotid artery
GFAP	Glial fibrillary acidic protein
HRP	Horseradish peroxidase
ICA	Internal carotid artery
MCAO	Middle cerebral artery occlusion
MPO	Myeloperoxidase
NANO-CAT/SOD	Nanoparticles loaded with catalase or superoxide dismutase
NPs	Nanoparticles
NPCs	Neural precursor cells (stem and progenitor cells)
PBS	Phosphate-buffered saline
PLGA	Poly (D,L-lactide *co*-glycolide)
PVA	Polyvinyl alcohol
RGL	Radial glia-like
RMS	Rostral migratory stream
ROS	Reactive oxygen species
RSA	Rat serum albumin
RT	Room temperature
SOD	Superoxide dismutase
SVZ	Subventricular zone
tPA	(recombinant human) Tissue-type plasminogen activator
VZ	Ventricular zone
IHC	Immuno Histochemistry
IF	Immuno Fluorescence

References

1. Gibson CL. Cerebral ischemic stroke: is gender important? Journal of Cerebral Blood Flow & Metabolism. 2013; 33:1355–61. [PubMed: 23756694]

2. Moskowitz MA, Lo EH, Iadecola C. The science of stroke: mechanisms in search of treatments. Neuron. 2010; 67:181–98. [PubMed: 20670828]

3. Dancause N. Vicarious function of remote cortex following stroke: recent evidence from human and animal studies. The Neuroscientist. 2006; 12:489–99. [PubMed: 17079515]

4. Jickling GC, Liu D, Stamova B, Ander BP, Zhan X, Lu A, et al. Hemorrhagic transformation after ischemic stroke in animals and humans. Journal of Cerebral Blood Flow & Metabolism. 2014; 34:185–99. [PubMed: 24281743]

5. Villarán RF, de Pablos RM, Argüelles S, Espinosa-Oliva AM, Tomás-Camardiel M, Herrera AJ, et al. The intranigral injection of tissue plasminogen activator induced blood–brain barrier disruption, inflammatory process and degeneration of the dopaminergic system of the rat. Neurotoxicology. 2009; 30:403–13. [PubMed: 19442825]

6. Wahlgren N, Ahmed N, Dávalos A, Hacke W, Millán M, Muir K, et al. Thrombolysis with alteplase 3–4· 5 h after acute ischaemic stroke (SITS-ISTR): an observational study. The Lancet. 2008; 372:1303–9.

7. Lewen A, Matz P, CHAN PH. Free radical pathways in CNS injury. Journal of neurotrauma. 2000; 17:871–90. [PubMed: 11063054]

8. Uttara B, Singh AV, Zamboni P, Mahajan R. Oxidative stress and neurodegenerative diseases: a review of upstream and downstream antioxidant therapeutic options. Current neuropharmacology. 2009; 7:65–74. [PubMed: 19721819]

9. Rodrigo R, Libuy M, Feliú F, Hasson D. Oxidative stress-related biomarkers in essential hypertension and ischemia-reperfusion myocardial damage. Disease markers. 2013; 35:773–90. [PubMed: 24347798]

10. Chen S-D, Yang D-I, Lin T-K, Shaw F-Z, Liou C-W, Chuang Y-C. Roles of oxidative stress, apoptosis, PGC-1α and mitochondrial biogenesis in cerebral ischemia. International journal of molecular sciences. 2011; 12:7199–215. [PubMed: 22072942]

11. Kennea NL, Mehmet H. Neural stem cells. The Journal of pathology. 2002; 197:536–50. [PubMed: 12115869]

12. Urbán N, Guillemot F. Neurogenesis in the embryonic and adult brain: same regulators, different roles. Frontiers in cellular neuroscience. 2014; 8:396. [PubMed: 25505873]

13. Dibajnia P, Morshead CM. Role of neural precursor cells in promoting repair following stroke. Acta Pharmacologica Sinica. 2013; 34:78–90. [PubMed: 23064725]

14. Dooley D, Vidal P, Hendrix S. Immunopharmacological intervention for successful neural stem cell therapy: New perspectives in CNS neurogenesis and repair. Pharmacology & therapeutics. 2014; 141:21–31. [PubMed: 23954656]

15. Kahle MP, Bix GJ. Neuronal Restoration Following Ischemic Stroke Influences, Barriers, and Therapeutic Potential. Neurorehabilitation and neural repair. 2013; 27:469–78. [PubMed: 23392917]

16. Huang T-T, Zou Y, Corniola R. Oxidative stress and adult neurogenesis—effects of radiation and superoxide dismutase deficiency. Seminars in cell & developmental biology. 2012; 23:738–44. [PubMed: 22521481]

17. Reddy MK, Labhasetwar V. Nanoparticle-mediated delivery of superoxide dismutase to the brain: an effective strategy to reduce ischemia-reperfusion injury. FASEB journal : official publication of the Federation of American Societies for Experimental Biology. 2009; 23:1384–95. [PubMed: 19124559]

18. Singhal A, Morris VB, Labhasetwar V, Ghorpade A. Nanoparticle-mediated catalase delivery protects human neurons from oxidative stress. Cell death & disease. 2013; 4:e903. [PubMed: 24201802]

19. Jaffer H, Adjei IM, Labhasetwar V. Optical imaging to map blood-brain barrier leakage. Scientific reports. 2013; 3:3117. [PubMed: 24178124]

20. Liu Y, Namba T, Liu J, Suzuki R, Shioda S, Seki T. Glial fibrillary acidic protein-expressing neural progenitors give rise to immature neurons via early intermediate progenitors expressing both glial fibrillary acidic protein and neuronal markers in the adult hippocampus. Neuroscience. 2010; 166:241–51. [PubMed: 20026190]

21. Barone F, Schmidt D, Hillegass L, Price W, White R, Feuerstein G, et al. Reperfusion increases neutrophils and leukotriene B4 receptor binding in rat focal ischemia. Stroke. 1992; 23:1337–47. [PubMed: 1381529]
22. Kharitonova TV, Melo TP, Andersen G, Egido JA, Castillo J, Wahlgren N. Importance of cerebral artery recanalization in patients with stroke with and without neurological improvement after intravenous thrombolysis. Stroke. 2013; 44:2513–8. [PubMed: 23881960]
23. Murphy TH, Corbett D. Plasticity during stroke recovery: from synapse to behaviour. Nature Reviews Neuroscience. 2009; 10:861–72. [PubMed: 19888284]
24. Ginsberg MD. Neuroprotection for ischemic stroke: past, present and future. Neuropharmacology. 2008; 55:363–89. [PubMed: 18308347]
25. Werner C. Neuroprotection in acute cerebral ischemia: Can we improve clinical outcomes? Best Practice & Research Clinical Anaesthesiology. 2010; 24:vii–x. [PubMed: 21619860]
26. Garber K. Stroke treatment—light at the end of the tunnel? Nature biotechnology. 2007; 25:838–40.
27. Reddy MK, Wu L, Kou W, Ghorpade A, Labhasetwar V. Superoxide dismutase-loaded PLGA nanoparticles protect cultured human neurons under oxidative stress. Applied biochemistry and biotechnology. 2008; 151:565–77. [PubMed: 18509606]
28. Peters O, Back T, Lindauer U, Busch C, Megow D, Dreier J, et al. Increased formation of reactive oxygen species after permanent and reversible middle cerebral artery occlusion in the rat. Journal of Cerebral Blood Flow & Metabolism. 1998; 18:196–205. [PubMed: 9469163]
29. Allen C, Bayraktutan U. Oxidative stress and its role in the pathogenesis of ischaemic stroke. International journal of stroke. 2009; 4:461–70. [PubMed: 19930058]
30. Aronowski J, Strong R, Grotta JC. Reperfusion injury: demonstration of brain damage produced by reperfusion after transient focal ischemia in rats. Journal of Cerebral Blood Flow & Metabolism. 1997; 17:1048–56. [PubMed: 9346429]
31. Kalogeris T, Bao Y, Korthuis RJ. Mitochondrial reactive oxygen species: a double edged sword in ischemia/reperfusion vs preconditioning. Redox biology. 2014; 2:702–14. [PubMed: 24944913]
32. Amantea D, Marrone MC, Nistico R, Federici M, Bagetta G, Bernardi G, et al. Oxidative stress in stroke pathophysiology: Validation of hydrogen peroxide metabolism as a pharmacological target to afford neuroprotection. International review of neurobiology. 2009; 85:363–74. [PubMed: 19607981]
33. Francis JW, Ren J, Warren L, Brown RH, Finklestein SP. Postischemic infusion of Cu/Zn superoxide dismutase or SOD: Tet451 reduces cerebral infarction following focal ischemia/reperfusion in rats. Experimental neurology. 1997; 146:435–43. [PubMed: 9270054]
34. Tsubokawa T, Jadhav V, Solaroglu I, Shiokawa Y, Konishi Y, Zhang JH. Lecithinized superoxide dismutase improves outcomes and attenuates focal cerebral ischemic injury via antiapoptotic mechanisms in rats. Stroke. 2007; 38:1057–62. [PubMed: 17272760]
35. Veronese FM, Caliceti P, Schiavon O, Sergi M. Polyethylene glycol–superoxide dismutase, a conjugate in search of exploitation. Advanced drug delivery reviews. 2002; 54:587–606. [PubMed: 12052716]
36. Panyam J, ZHOU W-Z, PRABHA S, SAHOO SK, LABHASETWAR V. Rapid endo-lysosomal escape of poly (DL-lactide-co-glycolide) nanoparticles: implications for drug and gene delivery. FASEB journal : official publication of the Federation of American Societies for Experimental Biology. 2002; 16:1217–26. [PubMed: 12153989]
37. Vieira HL, Alves PM, Vercelli A. Modulation of neuronal stem cell differentiation by hypoxia and reactive oxygen species. Progress in neurobiology. 2011; 93:444–55. [PubMed: 21251953]
38. Yun X, Maximov VD, Yu J, Zhu H, Vertegel AA, Kindy MS. Nanoparticles for targeted delivery of antioxidant enzymes to the brain after cerebral ischemia and reperfusion injury. Journal of Cerebral Blood Flow & Metabolism. 2013; 33:583–92. [PubMed: 23385198]
39. Takamiya M, Miyamoto Y, Yamashita T, Deguchi K, Ohta Y, Abe K. Strong neuroprotection with a novel platinum nanoparticle against ischemic stroke-and tissue plasminogen activator-related brain damages in mice. Neuroscience. 2012; 221:47–55. [PubMed: 22766232]
40. und Halbach, OvB. Immunohistological markers for staging neurogenesis in adult hippocampus. Cell and tissue research. 2007; 329:409–20. [PubMed: 17541643]

41. Bonaguidi MA, Wheeler MA, Shapiro JS, Stadel RP, Sun GJ, Ming G-l, et al. In vivo clonal analysis reveals self-renewing and multipotent adult neural stem cell characteristics. Cell. 2011; 145:1142–55. [PubMed: 21664664]
42. Lichtenwalner RJ, Parent JM. Adult neurogenesis and the ischemic forebrain. Journal of Cerebral Blood Flow & Metabolism. 2006; 26:1–20. [PubMed: 15959458]
43. Corbin JG, Gaiano N, Juliano SL, Poluch S, Stancik E, Haydar TF. Regulation of neural progenitor cell development in the nervous system. Journal of neurochemistry. 2008; 106:2272–87. [PubMed: 18819190]
44. Wojakowski W, Ratajczak M, Tendera M. Mobilization of very small embryonic-like stem cells in acute coronary syndromes and stroke. Herz. 2010; 35:467–73. [PubMed: 20981396]
45. Chen S-H, Wang J-J, Chen C-H, Chang H-K, Lin M-T, Chang F-M, et al. Umbilical cord blood-derived CD34+ cells improve outcomes of traumatic brain injury in rats by stimulating angiogenesis and neurogenesis. Cell transplantation. 2014; 23:959–79. [PubMed: 23582375]
46. Kam M, Curtis MA, McGlashan SR, Connor B, Nannmark U, Faull RL. The cellular composition and morphological organization of the rostral migratory stream in the adult human brain. Journal of chemical neuroanatomy. 2009; 37:196–205. [PubMed: 19159677]
47. Wang C, Liu F, Liu Y-Y, Zhao C-H, You Y, Wang L, et al. Identification and characterization of neuroblasts in the subventricular zone and rostral migratory stream of the adult human brain. Cell research. 2011; 21:1534–50. [PubMed: 21577236]
48. Achuta VS, Rezov V, Uutela M, Louhivuori V, Louhivuori L, Castren ML. Tissue plasminogen activator contributes to alterations of neuronal migration and activity-dependent responses in fragile X mice. J Neurosci. 2014; 34:1916–23. [PubMed: 24478370]
49. Del Zoppo GJ. Investigational use of tPA in acute stroke. Annals of emergency medicine. 1988; 17:1196–201. [PubMed: 3142317]
50. Niessen F, Hilger T, Hoehn M, Hossmann K-A. Thrombolytic Treatment of Clot Embolism in Rat Comparison of Intra-arterial and Intravenous Application of Recombinant Tissue Plasminogen Activator. Stroke. 2002; 33:2999–3005. [PubMed: 12468803]
51. Perez-Pinzon MA, Dave KR, Raval AP. Role of reactive oxygen species and protein kinase C in ischemic tolerance in the brain. Antioxidants & redox signaling. 2005; 7:1150–7. [PubMed: 16115018]
52. Shichita T, Ago T, Kamouchi M, Kitazono T, Yoshimura A, Ooboshi H. Novel therapeutic strategies targeting innate immune responses and early inflammation after stroke. Journal of neurochemistry. 2012; 123:29–38. [PubMed: 23050640]
53. Macrez R, Ali C, Toutirais O, Le Mauff B, Defer G, Dirnagl U, et al. Stroke and the immune system: from pathophysiology to new therapeutic strategies. The Lancet Neurology. 2011; 10:471–80. [PubMed: 21511199]
54. Murikinati S, Jüttler E, Keinert T, Ridder DA, Muhammad S, Waibler Z, et al. Activation of cannabinoid 2 receptors protects against cerebral ischemia by inhibiting neutrophil recruitment. FASEB journal : official publication of the Federation of American Societies for Experimental Biology. 2010; 24:788–98. [PubMed: 19884325]
55. Cuartero MI, Ballesteros I, Moraga A, Nombela F, Vivancos J, Hamilton JA, et al. N2 neutrophils, novel players in brain inflammation after stroke modulation by the PPARγ agonist rosiglitazone. Stroke. 2013; 44:3498–508. [PubMed: 24135932]
56. Varma MR, Varga AJ, Knipp BS, Sukheepod P, Upchurch GR, Kunkel SL, et al. Neutropenia impairs venous thrombosis resolution in the rat. Journal of vascular surgery. 2003; 38:1090–8. [PubMed: 14603221]
57. Friedrich V, Flores R, Muller A, Bi W, Peerschke E, Sehba FA. Reduction of neutrophil activity decreases early microvascular injury after subarachnoid haemorrhage. J Neuroinflammation. 2011; 8:2094–8.
58. Fraser PA. The role of free radical generation in increasing cerebrovascular permeability. Free Radical Biology and Medicine. 2011; 51:967–77. [PubMed: 21712087]
59. Pun PB, Lu J, Moochhala S. Involvement of ROS in BBB dysfunction. Free radical research. 2009; 43:348–64. [PubMed: 19241241]

60. Al Ahmad A, Gassmann M, Ogunshola OO. Involvement of oxidative stress in hypoxia-induced blood–brain barrier breakdown. Microvascular research. 2012; 84:222–5. [PubMed: 22668821]

61. Copin JC, Bengualid DJ, Da Silva RF, Kargiotis O, Schaller K, Gasche Y. Recombinant tissue plasminogen activator induces blood–brain barrier breakdown by a matrix metalloproteinase-9-independent pathway after transient focal cerebral ischemia in mouse. European Journal of Neuroscience. 2011; 34:1085–92. [PubMed: 21895804]

62. Obermeier B, Daneman R, Ransohoff RM. Development, maintenance and disruption of the blood-brain barrier. Nature medicine. 2013; 19:1584–96.

63. Uttara B, Singh AV, Zamboni P, Mahajan RT. Oxidative stress and neurodegenerative diseases: a review of upstream and downstream antioxidant therapeutic options. Curr Neuropharmacol. 2009; 7:65–74. [PubMed: 19721819]

64. Kolb B, Morshead C, Gonzalez C, Kim M, Gregg C, Shingo T, et al. Growth factor-stimulated generation of new cortical tissue and functional recovery after stroke damage to the motor cortex of rats. Journal of Cerebral Blood Flow & Metabolism. 2007; 27:983–97. [PubMed: 16985505]

65. Sun Y, Jin K, Xie L, Childs J, Mao XO, Logvinova A, et al. VEGF-induced neuroprotection, neurogenesis, and angiogenesis after focal cerebral ischemia. Journal of Clinical Investigation. 2003; 111:1843. [PubMed: 12813020]

66. Kennedy KA, Sandiford SD, Skerjanc IS, Li SS-C. Reactive oxygen species and the neuronal fate. Cellular and Molecular Life Sciences. 2012; 69:215–21. [PubMed: 21947442]

67. Krupinski J, Kaluza J, Kumar P, Kumar S, Wang JM. Role of angiogenesis in patients with cerebral ischemic stroke. Stroke. 1994; 25:1794–8. [PubMed: 7521076]

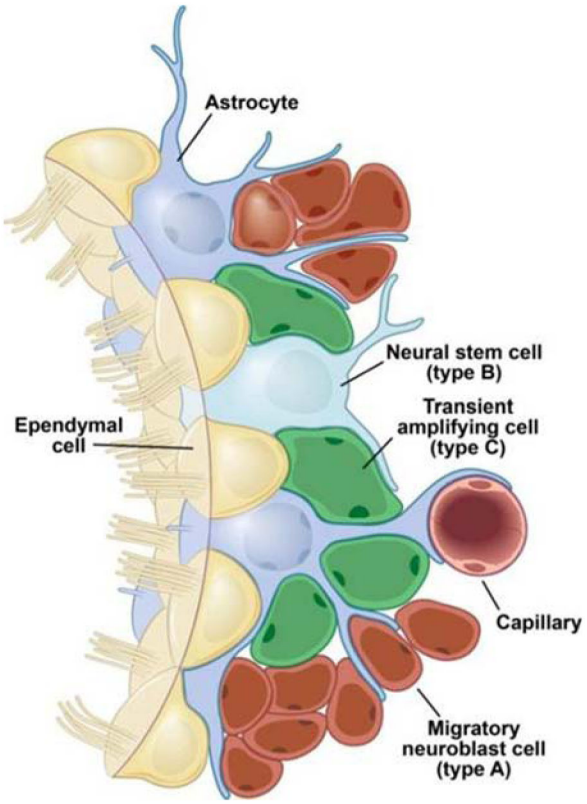

Figure 1. Schematic representing various stem and glial cells associated with the inherent process of neurogenesis in post-stroke conditions

The figure illustrates the “inherent neurogenesis” concept, achieved by various stem cell types and glial cells, typically associated with spontaneous self-recovery after stroke.

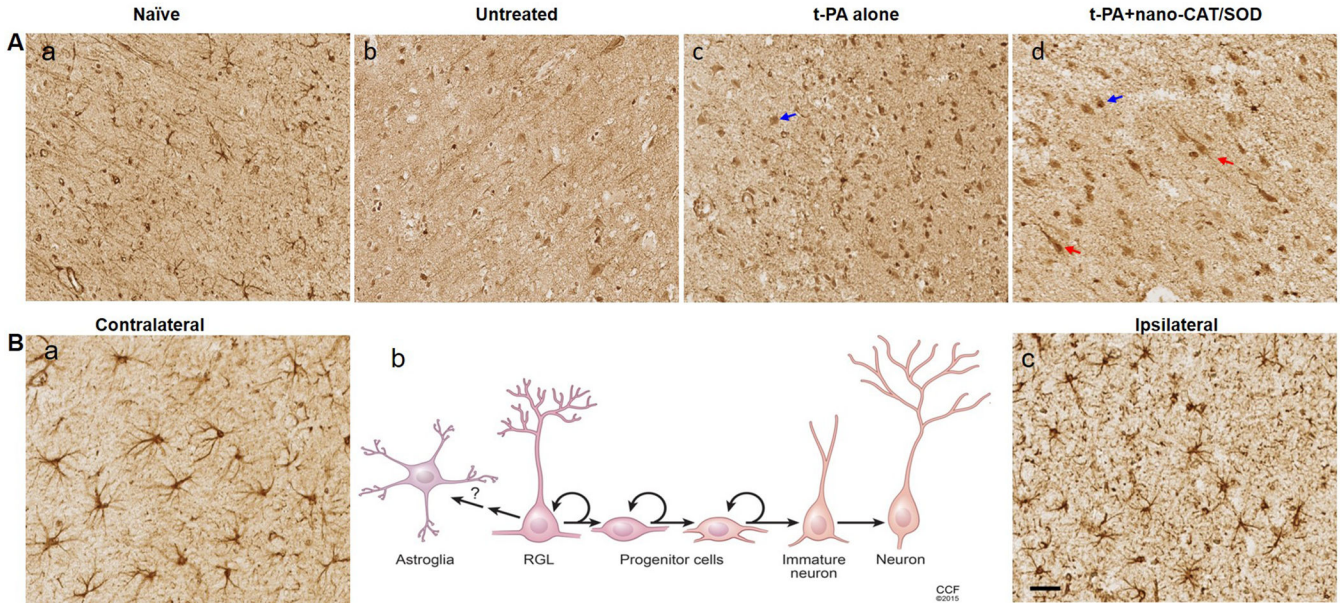

Figure 2. Immunohistochemical analysis of brain sections for GFAP-expressing astrocytes, progenitor cells and radial glia-like (RGL) cells

Following embolic stroke, animals received different treatments at 3 h and brains were collected 48 h post stroke. Brain sections were stained for GFAP expression. Besides the astrocytes, the GFAP staining also showed various cell types in naïve (A–a), untreated (A–b), tPA-treated (A–c), and tPA + nano-CAT/SOD-treated (A–d) animals. Animals treated with tPA (A–c, blue arrow) and tPA + nano-CAT/SOD (A–d, blue arrow) show round progenitor cells; those treated with tPA + nano-CAT/SOD also show RGL cells (A–d, red arrows). In the GFAP stained brain sections, the astrocyte morphology observed on the ipsilateral and contralateral sides was compared between various groups. The contralateral side (B–a) exhibits normal astrocyte morphology with characteristic star-shaped long extensions, whereas the ipsilateral side (B–c) exhibits astrocytosis, as is evidenced by the altered morphology (swollen and thickened processes, increased GFAP expression). The schematic (B–b) provides a morphological display of the various cell types associated with neurogenesis to provide a comparison of the associated cells vs. the GFAP-positive round progenitor cells and RGL cells. Scale bar = 50 μm. Representative brain section images from three animals in each group are shown.

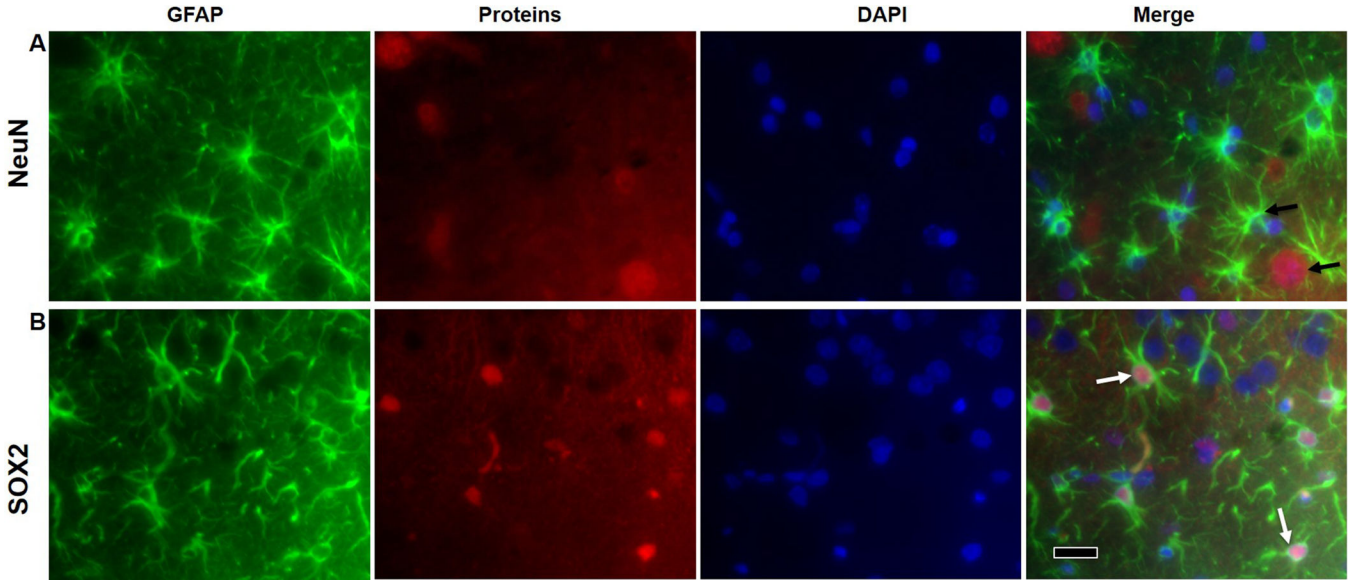

Figure 3. Immunofluorescence for detection of GFAP-expressing astrocytes, NPCs and RGL cells

To further elucidate the GFAP positive cell types from the DAB-IHC, brain tissue from tPA-nano-CAT/SOD treated animals were co-stained for marker of GFAP, mature neuron (NeuN) and neural progenitors (SOX2). The GFAP positive cells on the contralateral side exhibits normal astrocyte morphology with characteristic star-shaped long extensions and does not co-stain with NeuN (A, black arrows), whereas the ipsilateral ischemic brain exhibits astrocytosis and altered morphology (lacking astrocytic morphology) and co-stained GFAP with SOX2 (B, white arrows), suggesting the presence of progenitor cells. Scale bar = 20 μm.

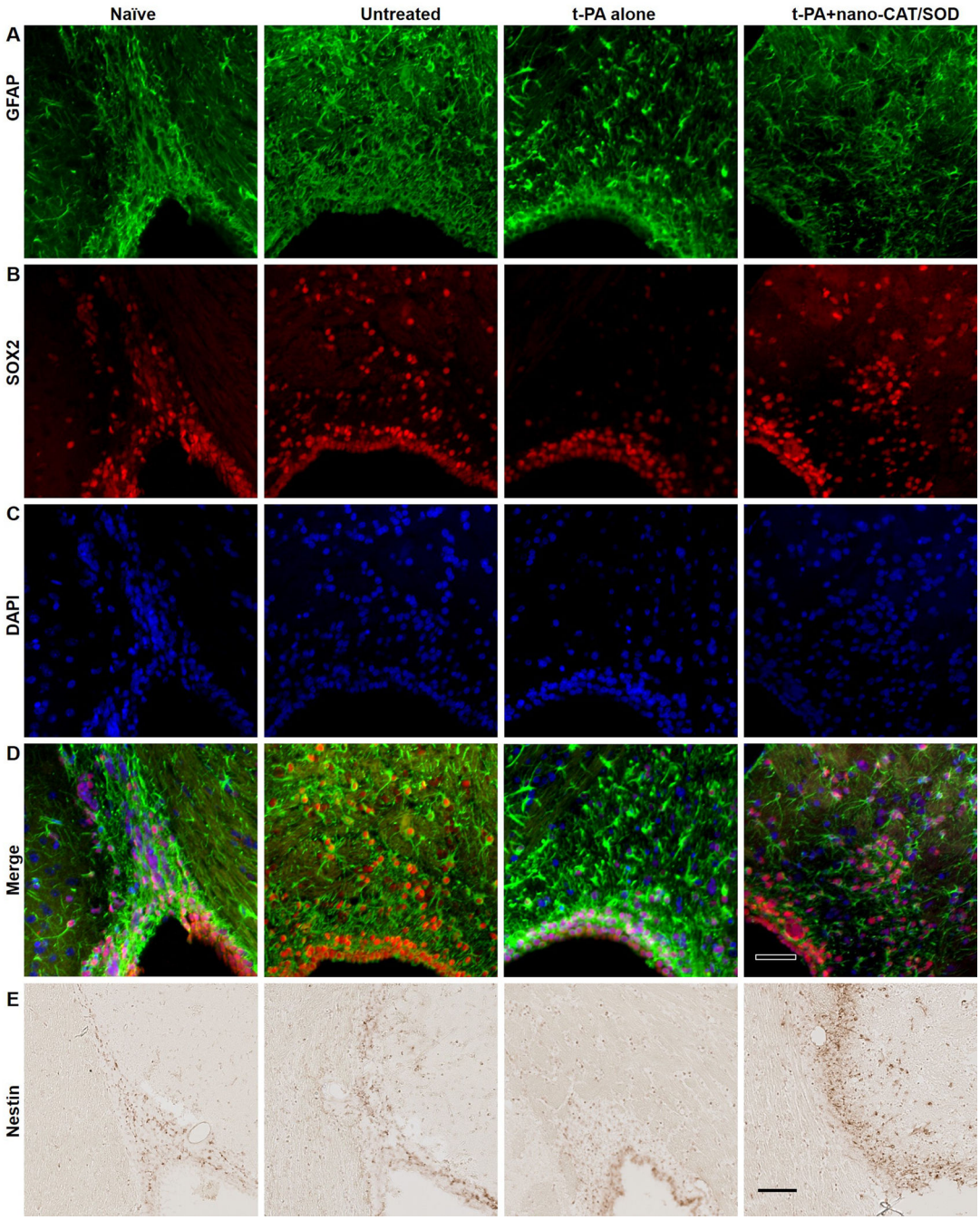

Figure 4. Immunohistochemical analysis for GFAP, SOX2, and Nestin for neuronal progenitor cells (NPCs) in the SVZ and RMS

The NPCs could be detected with Nestin (in NPCs and transition astroglia), GFAP (in astrocytes and NPCs), and SOX2 (in non-radial neural progenitors) in IHC. The brain sections of naïve showed staining for GFAP, Nestin, and SOX2 in both SVZ and RMS. The expression of these NPCs related proteins increased after stroke as shown in the untreated sections; however, the expression of SOX2 and Nestin is reduced in RMS after the treatment with tPA alone. The treatment with tPA + nano-CAT/SOD increased the expression of GFAP, Nestin, and SOX2 than in naïve and tPA alone treated animals. Scale bar = 50 μm.

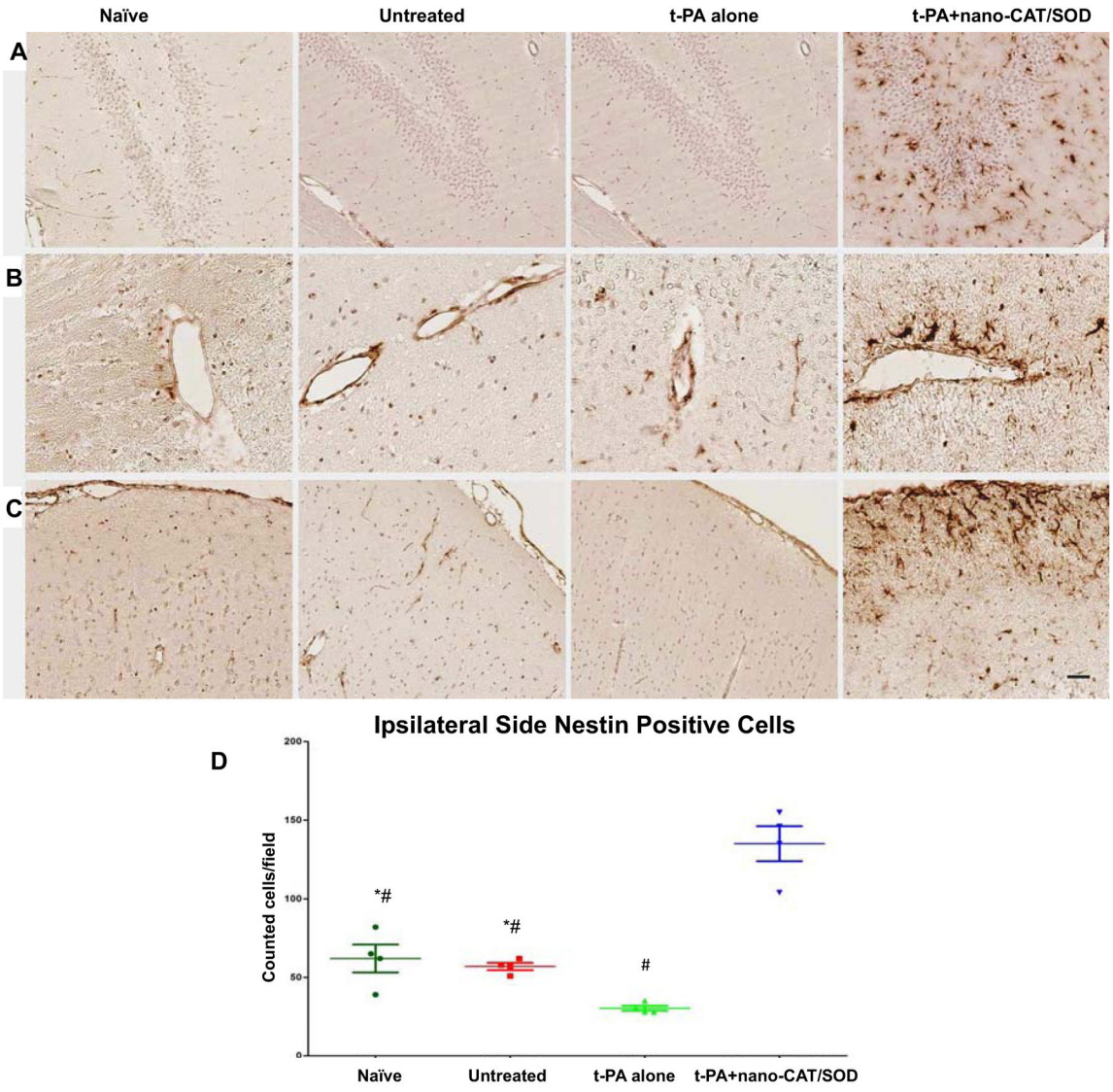

Figure 5. Immunohistochemical analysis of brain sections for nestin-positive neural progenitors

Following embolic stroke, animals received different treatments at 3 h, and brains were collected at 48 h post stroke from groups of naïve, untreated, tPA alone, and tPA + nano-CAT/SOD treated animals. Brain sections were stained for nestin expression in the hippocampus (A), tissues around the blood vessel (B), and cortex (C). Brains from rats treated with tPA + nano-CAT/SOD show increased nestin expression in the hippocampus, blood vessels, and cortex from the ipsilateral side than the brain sections from naïve, untreated, and tPA-alone animals (D). Animals receiving tPA + nano-CAT/SOD showed strong nestin-expressing cells entering from the blood vessels (B) and meninges (C). * significant difference ($p<0.05$) as compared to tPA; # significant difference ($p<0.05$) as compared to tPA+ nano-CAT/SOD. Scale bar = 50 μm.

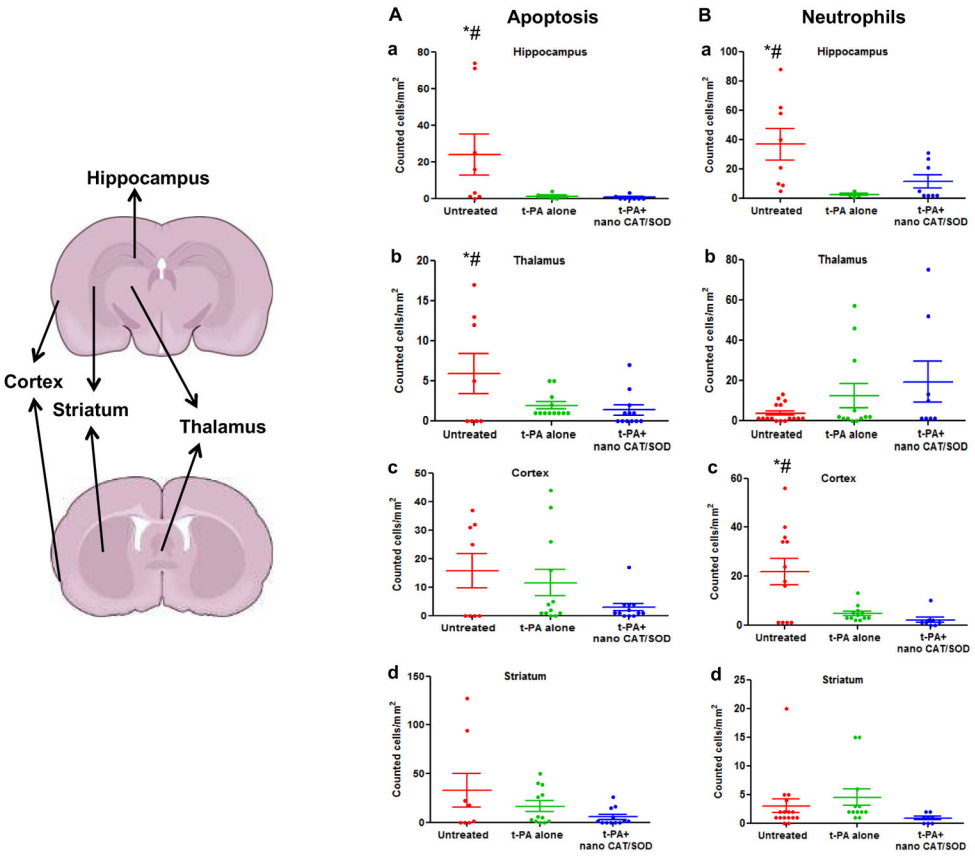

Figure 6. Quantification of apoptotic cells and infiltrating neutrophils in different regions of the brain

Overall there is reduction in apoptotic cells in tPA+ nano-CAT/SOD treatment than in untreated and tPA alone groups. Neutrophil infiltration is also suppressed in the cortex of tPA+ nano-CAT/SOD brains vs. untreated and t-PA alone treated animal brain sections. * significant difference ($p<0.05$) as compared to tPA; # significant difference ($p<0.05$) as compared to tPA+ nano-CAT/SOD.

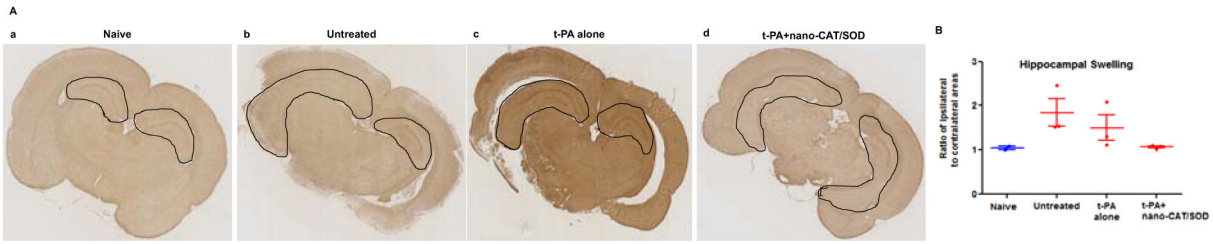

Figure 7. Immunohistochemical analysis of brain sections for hippocampus swelling

Following embolic stroke, animals received different treatments at 3 h, and brains were collected at 48 h post stroke. Brain sections were stained for GFAP. (A) Animals treated with tPA + nano-CAT/SOD show reduced swelling in the hippocampus than untreated and tPA alone treated animals. (B) Ratio of the ipsilateral to contralateral hippocampal areas showed reduced hippocampal swelling in tPA + CAT/SOD treated than in other groups. Data as mean ± s.e.m, naïve = 2, other groups = 3 animals in each group. $p = 0.06$ for untreated vs. tPA+ nano-CAT/SOD treated; $p = 0.13$ for tPA alone vs. tPA+ nano-CAT/SOD treated.

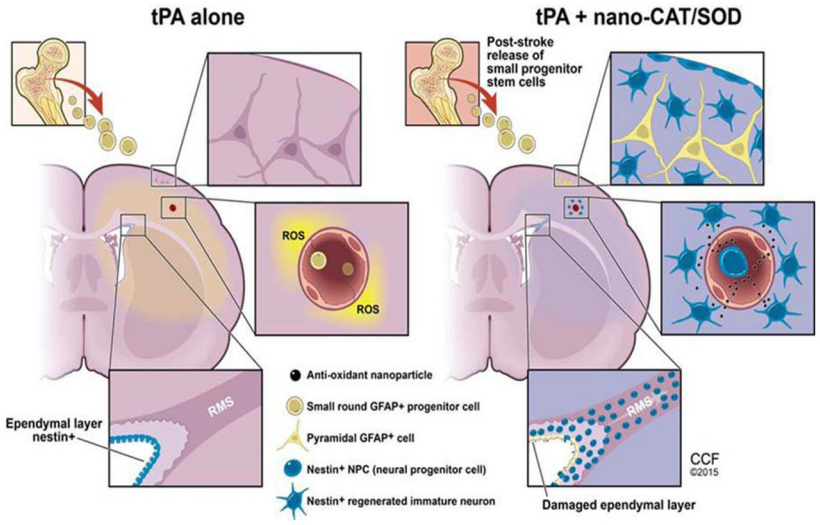

Figure 8. Schematic representation of the proposed mechanism for the efficacy of tPA + nano-CAT/SOD

The illustration demonstrates how neutralizing ROS with nano-CAT/SOD promotes progenitor cell activation and migration in the ischemic tissue in the post-stroke rat brain.